Title
Stimulation of Hair Growth by Small Molecules that Activate Autophagy

Permalink
https://escholarship.org/uc/item/7pt84554

Journal
Cell Reports, 27(12)

ISSN
2639-1856

Authors
Chai, Min
Jiang, Meisheng
Vergnes, Laurent
et al.

Publication Date
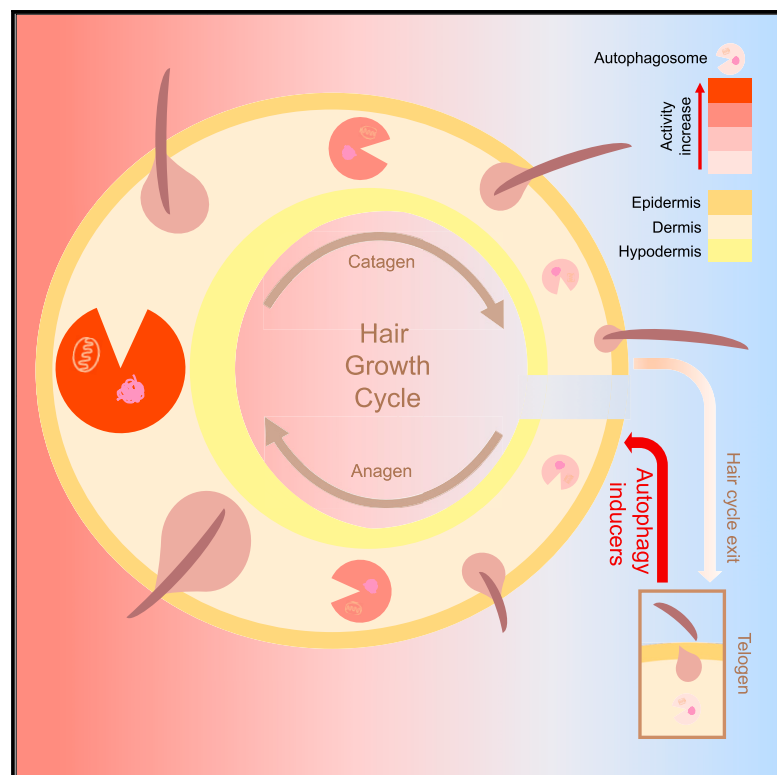2019-06-01

DOI
10.1016/j.celrep.2019.05.070

Peer reviewed

Stimulation of Hair Growth by Small Molecules that Activate Autophagy

Graphical Abstract

Authors

Min Chai, Meisheng Jiang,
Laurent Vergnes, ..., Gay M. Crooks,
Karen Reue, Jing Huang

Correspondence

jinghuang.ucla@gmail.com

In Brief

Hair regeneration requires reactivating dormant hair follicle stem cells. Chai et al. discover that pharmacological induction of autophagy is sufficient to activate quiescent telogen hair follicles, initiating new anagen hair growth. Hair loss resulting from shortened anagen, lengthened telogen, and/or impeded anagen induction may thereby be rescued by activating autophagy.

Highlights

- mTOR and AMPK modulation by rapamycin, metformin, and α-KG induces anagen hair growth

- Autophagy induction is necessary and sufficient for anagen entry and hair growth

- Autophagy is increased during anagen phase of the natural hair follicle cycle

- Aged mice fed the autophagy-inducing metabolite α-KB are protected from hair loss

Report

Stimulation of Hair Growth by Small Molecules that Activate Autophagy

Min Chai,[1] Meisheng Jiang,[2] Laurent Vergnes,[3] Xudong Fu,[2] Stéphanie C. de Barros,[4] Ngan B. Doan,[4] Wilson Huang,[2] Jessie Chu,[2] Jing Jiao,[2] Harvey Herschman,[2,5,6] Gay M. Crooks,[4,6] Karen Reue,[3,5] and Jing Huang[2,5,6,7,*]

[1]Molecular Biology Interdisciplinary Graduate Program, University of California, Los Angeles, Los Angeles, CA 90095, USA
[2]Department of Molecular and Medical Pharmacology, David Geffen School of Medicine, University of California, Los Angeles, Los Angeles, CA 90095, USA
[3]Department of Human Genetics, David Geffen School of Medicine, University of California, Los Angeles, Los Angeles, CA 90095, USA
[4]Department of Pathology and Laboratory Medicine, David Geffen School of Medicine, University of California, Los Angeles, Los Angeles, CA 90095, USA
[5]Molecular Biology Institute, University of California, Los Angeles, Los Angeles, CA 90095, USA
[6]Jonsson Comprehensive Cancer Center, University of California, Los Angeles, Los Angeles, CA 90095, USA
[7]Lead Contact
*Correspondence: jinghuang.ucla@gmail.com
https://doi.org/10.1016/j.celrep.2019.05.070

SUMMARY

Hair plays important roles, ranging from the conservation of body heat to the preservation of psychological well-being. Hair loss or alopecia affects millions worldwide, but methods that can be used to regrow hair are lacking. We report that quiescent (telogen) hair follicles can be stimulated to initiate anagen and hair growth by small molecules that activate autophagy, including the metabolites α-ketoglutarate (α-KG) and α-ketobutyrate (α-KB), and the prescription drugs rapamycin and metformin, which impinge on mTOR and AMPK signaling. Stimulation of hair growth by these agents is blocked by specific autophagy inhibitors, suggesting a mechanistic link between autophagy and hair regeneration. Consistently, increased autophagy is detected upon anagen entry during the natural hair follicle cycle, and oral α-KB prevents hair loss in aged mice. Our finding that anagen can be pharmacologically activated in telogen skin when natural anagen-inducing signal(s) are absent has implications for the treatment of hair loss patients.

INTRODUCTION

The biological and psychological importance of hair is well recognized. Hair loss affects millions worldwide and can occur because of aging, hormonal dysfunction, or autoimmunity or as a side effect of cancer treatment. Mammalian hair growth consists of cyclic repetitions of telogen (quiescence), anagen (regeneration), and catagen (degeneration) phases of the hair follicle (Müller-Röver et al., 2001; Schneider et al., 2009). This hair follicle cycle is regulated by both intrinsic and extrinsic signals that control quiescence and activation of hair follicle stem cells (HFSCs). Inadequate hair follicle stem cell activation and proliferation underlie alopecia in numerous biological and pathological

conditions, including aging (Gilhar et al., 2012; Petukhova et al., 2010; Keyes et al., 2013; Chueh et al., 2013). Molecules that can promote hair follicle stem cell activation and anagen initiation have been intensely searched for, as they may both help reveal how hair regeneration is regulated and provide therapeutic and cosmetic interventions. Here, we postulate that telogen hair follicles may be induced to enter anagen by pharmacologically triggering autophagy.

As a fundamental process for degrading and recycling cellular components, autophagy is critical for adaptation to nutrient starvation and other adverse environmental conditions, and it is regulated by such signals (Ohsumi, 2014; Galluzzi et al., 2014). Autophagy is also important for quality control of proteostasis through the elimination of misfolded or damaged proteins and damaged organelles. The loss of autophagy may be causally related to neurodegeneration and other diseases (Mizushima et al., 2008). Autophagy declines with age (Cuervo and Dice, 2000; Levine and Kroemer, 2008), likely contributing to the higher prevalence of autophagy-related diseases (e.g., cancer, neurodegenerative diseases) in the elderly. Autophagic clearing of active, healthy mitochondria in hematopoietic stem cells is required to maintain quiescence and stemness (Ho et al., 2017), and autophagy fulfills the nutrient demand of quiescent muscle stem cell activation (Tang and Rando, 2014). In the skin, autophagy is required for self-renewal and differentiation of epidermal and dermal stem cells (Salemi et al., 2012; Belleudi et al., 2014; Chikh et al., 2014), but its role in hair follicle stem cells has remained controversial. On one hand, autophagy may be required for hair growth as skin grafts from the autophagy-related gene 7 (Atg7)-deficient mice exhibit abnormal hair growth (Yoshihara et al., 2015). On the other hand, Atg7 deficiency in epithelial cells of the skin and hair was reported to be compatible with growth of hair, although sebaceous glands were affected, and male mutant mice developed an oily coat when they aged (Rossiter et al., 2018). It was also reported that psychological stress induced autophagy and delay of hair cycle (Wang et al., 2015).

Previously, alterations in intrinsic signaling, gene expression, and circadian function were implicated to prevent anagen entry in aged hair follicle stem cells and result in alopecia
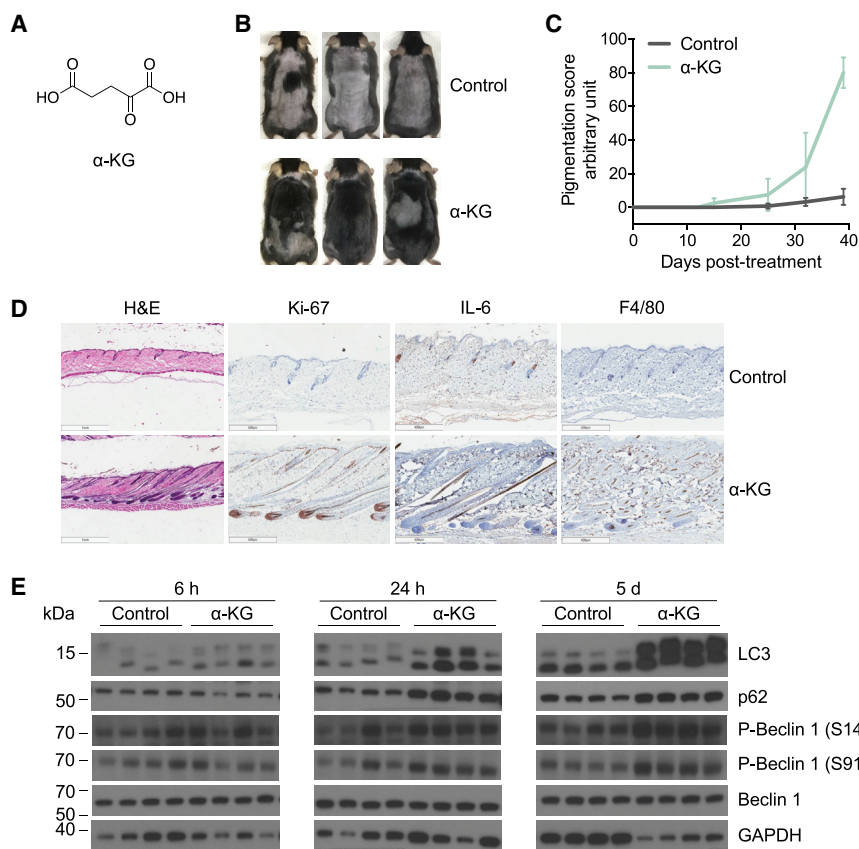
Figure 1. Hair Regeneration Is Induced by Topical Treatment with α-KG

(A) Structure of α-KG.

(B) α-KG induces hair regeneration. Male mice were shaved on postnatal day 44 (telogen) and topically treated with vehicle control (DMSO in ~250 μL PLO Base) or α-KG (dissolved in DMSO and then added to ~250 μL PLO Base at 32 mM final) every other day over 39 days. Melanin pigmentation in the skin of α-KG-treated animals, indicative of anagen induction by the treatment, became visible as early as day 12; vehicle-treated mice did not show significant pigmentation for at least 39 days. Hair growth from the pigmented skin areas of α-KG-treated mice was visible within 5–7 days. Photographs shown were taken on day 39 post-treatment, by which time mice treated with α-KG exhibited overall hair growth, whereas control mice still had no hair generally except for random hair patches on some animals. Total number of animals: control, n = 26; α-KG, n = 28. Similar effects by α-KG were seen in female mice (shown in Figure S1D).

(C) Quantification for appearance of melanin pigmentation (indicating onset of anagen) in mouse skin treated with α-KG versus control. Pigmentation scoring is described in STAR Methods. Number of animals shown in (A): control, n = 4; α-KG, n = 4. Data are represented as mean ± SD.

(D) Microphotographs of H&E-stained skin tissue sections from mice treated with 32 mM α-KG, showing new hair follicles and enlarged bulbs, elongated hair shafts, and thickened dermal layers. Hematoxylin is a basic dye that stains nucleic acids purplish blue; eosin is an acidic dye that stains cytoplasm and extracellular matrix (e.g., collagen) pink. Immunohistochemistry for Ki-67, a marker for cell proliferation (Magerl et al., 2001), further demonstrated the formation of new hair follicles. IL-6 and F4/80 are inflammatory cytokine and macrophage markers, respectively (Hirano et al., 1990; Wang et al., 2006). Controls for IL-6 and F4/80 positive inflammatory skin are shown in Figure S1E. Scale bars for H&E, 1 mm; scale bars for Ki-67, IL-6, and F4/80, 400 μm.

(E) Induction of autophagy-associated markers, including LC3, p62, and phosphorylated beclin 1, in telogen skin of mice treated with α-KG for 6 h, 24 h, and 5 days. Skin remained in telogen during the treatment period as confirmed by the lack of skin pigmentation. Each lane is from a different animal. Number of animals: four for each treatment.

See also Figure S1.

(Castilho et al., 2009; Keyes et al., 2013; Solanas et al., 2017). The unforeseen finding that supplementation of a metabolite α-ketobutyrate (α-KB) in old mice can increase longevity and prevent alopecia (Huang et al., 2016) suggests that rejuvenating aging or aging associated deficiencies may restore hair follicle stem cell function and hair growth in skin. We report herein that autophagy is increased during anagen phase of the natural hair follicle cycle and demonstrate that specific small molecules that induce autophagy can be used to promote anagen entry and hair growth from quiescent telogen phase.

RESULTS

Induction of autophagy is mediated by some of the same cellular energy metabolism regulators that have been linked to or implicated in the effect of dietary restriction (DR) on longevity. We previously showed that the metabolite α-ketoglutarate (α-KG) is induced upon dietary restriction and mediates its longevity effect in *C. elegans*. α-KG also increases autophagy in both worms and cultured mammalian cells (Chin et al., 2014). Here we tested whether α-KG can increase hair regeneration, using a commonly used *in vivo* C57BL/6J mouse dorsal skin model. We mainly tested the topical treatment method, as it is most easily translated to human patients. Minoxidil, a vasodilator used to treat pattern hair loss (Messenger and Rundegren, 2004), was included for comparison because it has typically been used as a positive control in much hair research (Figure S1A). Male mice at 6.5 weeks of age (postnatal day 44) were shaved on the back, when dorsal skin hair follicles are in telogen (Müller-Röver et al., 2001). α-KG or vehicle control treatment was applied topically every other day. α-KG treatment drastically enhances hair regeneration (Figures 1A and 1B). Anagen in black mice is macroscopically recognizable by the melanin pigment visible through the skin, as the melanogenic activity of follicular melanocytes is strictly coupled to the anagen stage of the hair cycle (Slominski and Paus, 1993). In the experiment shown in Figure 1B, skin pigmentation was visible by day 12 post-treatment with α-KG (Figure 1C). In
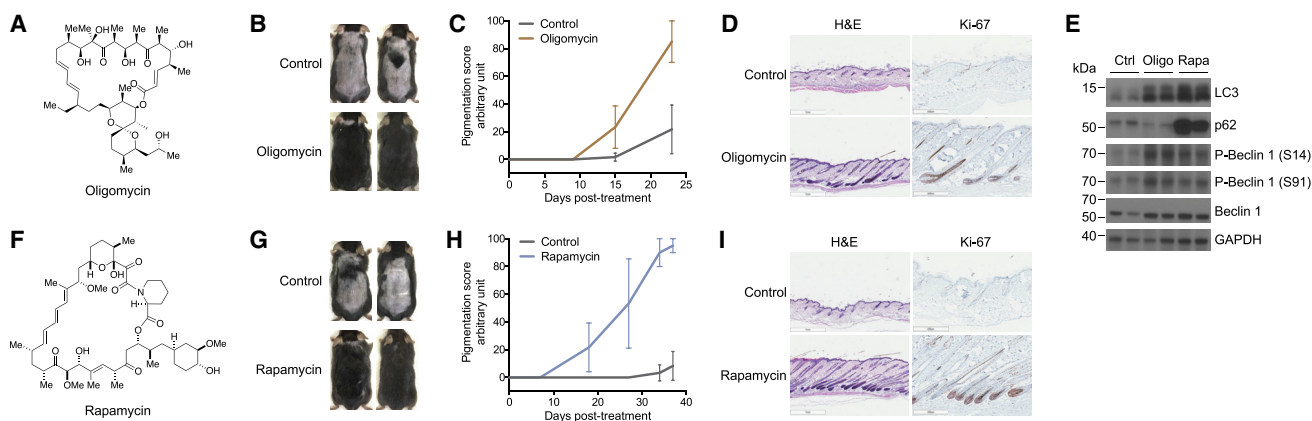
Figure 2. Hair Regeneration Is Induced by Topical Treatment with Oligomycin and Rapamycin

(A) Structure of oligomycin.

(B) Oligomycin (100 μM) induces hair regeneration. Male mice were shaved on postnatal day 44 and topically treated every other day. Photographs shown were taken on day 23 post-treatment. Number of animals: control, n = 23; oligomycin, n = 23. Similar effects by oligomycin were seen in female mice (Figure S1D).

(C) Quantification for appearance of melanin pigmentation in mouse skin treated with oligomycin versus control. Number of animals: control, n = 3; oligomycin, n = 3. Data are represented as mean ± SD.

(D) Microphotographs of H&E- and Ki-67-stained skin tissue section from mice treated with 100 μM oligomycin. Scale bars for H&E, 1 mm; scale bars for Ki-67, 400 μm.

(E) Western blot analysis of autophagy-related markers in telogen skin of mice treated 5 days with indicated compounds. Ctrl, control; Oligo, oligomycin; Rapa, rapamycin.

(F) Structure of rapamycin.

(G) Rapamycin (1.6 μM) induces hair regeneration. Male mice were shaved on postnatal day 43 and treated topically every other day. Photographs were taken on day 37 post-treatment. Number of animals: control, n = 18; rapamycin, n = 17. Rapamycin at 100 nM gave similar results as 1.6 μM (Figure S2). Similar effects by rapamycin were seen in female mice (Figure S2B). Rapamycin at 16 μM, however, resulted in hair loss and open wounds (data not shown), consistent with a previous vascular grafts study in rats receiving high-dose rapamycin (Walpoth et al., 2001); this may be due to more severe inhibition of mTOR, which was reported to be required for hair follicle stem cell activation (Castilho et al., 2009; Kellenberger and Tauchi, 2013; Deng et al., 2015).

(H) Quantification for appearance of melanin pigmentation in mouse skin treated with rapamycin (1.6 μM) versus control. Number of animals: control, n = 3; rapamycin, n = 3. Data are represented as mean ± SD.

(I) Microphotographs of H&E- and Ki-67-stained skin tissue section from mice shown in (G). Scale bars for H&E, 1 mm; scale bars for Ki-67, 400 μm.

See also Figure S2.

contrast, in vehicle-treated control mice, no pigmentation or only a few scattered pigmented spots were apparent at least until day 39, when animals were sacrificed for histological and biochemical analyses. Hair grew from the pigmented skin area of α-KG-treated mice within 5–7 days, and by day 39 post-treatment, α-KG-treated mice exhibited robust hair growth; in contrast, control mice showed little or no hair growth overall (Figure 1B). The effects of α-KG on anagen initiation and hair regeneration were even more dramatic when mice were treated later in telogen at 8 weeks of age (Figures S1B and S1C). α-KG stimulation of hair growth is gender independent; α-KG exhibited similar hair stimulating effects in female mice (Figure S1D).

Formation and differentiation of hair follicles in α-KG-treated mice were correspondingly demonstrated by histological analyses (Figure 1D). More follicles and high proliferation marker Ki-67 expression were observed in α-KG treatment group, showing anagen phase induction (Figure 1D). In telogen skin, α-KG initiated new anagen waves as early as day 7 post-treatment. Because inflammation and wound repair are known to stimulate tissue, including hair regeneration (Ito et al., 2007), our study was focused only on molecules that do not cause skin damage or other abnormal skin conditions. There was no evidence of skin irritation or inflammation by α-KG or other small-molecule treatments described in this study

(unless otherwise indicated) per visual inspection and confirmed by IL-6 and F4/80 staining (Figure 1D; Figure S1E).

Mice of the same age as those used for regeneration experiments were also acutely treated and analyzed for early biochemical changes. Increased autophagy induction in the α-KG-treated mouse skin was supported by western blot analysis of LC3 (Kabeya et al., 2000) at both 24 h and 5 days post-treatment (Figure 1E). Expression of the autophagy substrate p62/SQSTM1, which is widely used as an indicator of autophagic degradation, was also increased with autophagy induction by α-KG in the mouse skin (Figure 1E) as well as by rapamycin-induced autophagy (see below). This is likely due to compensation through up-regulation of p62 transcription (Figure S1F), as was reported for p62 during prolonged starvation (Sahani et al., 2014).

Longevity increase by α-KG was found to be mediated, at the molecular level, through direct inhibition of the highly conserved mitochondrial ATP synthase/ATPase (complex V) and subsequent decrease of target of rapamycin (TOR) activity downstream (Chin et al., 2014). We tested whether hair regeneration by α-KG may also be mediated by ATP synthase inhibition. Consistent with this mechanism, topical treatment with the complex V inhibitor oligomycin similarly promoted hair regeneration in both male (Figures 2A–2D) and female (Figure S1D) mice. Also, like α-KG, oligomycin treatment results in TOR inhibition

and autophagy activation (Chin et al., 2014). Here we also detected increased autophagy in topical oligomycin treated mouse skin, as indicated by LC3 expression (Figure 2E).

The TOR protein is a main mediator of the effect of dietary restriction in longevity. Inhibition of TOR (e.g., by rapamycin) elicits autophagy. We therefore asked whether rapamycin might also increase hair regeneration. As shown in Figures 2F–2I and Figure S2, topical rapamycin treatment accelerated hair regeneration, both visually and histologically. Autophagic LC3, p62, and mTOR-dependent phosphorylated beclin 1 S14 (Russell et al., 2013; Liang et al., 1999) were increased in rapamycin-treated mouse telogen skin (Figure 2E). Consistently, beclin 1 S14 phosphorylation was also increased in mouse skin by day 5 post-treatment with α-KG (Figure 1E) and oligomycin (Figure 2E). Together, these results show that hair regeneration can be accelerated by either indirect or direct inhibition of TOR pathway activity and induction of autophagy.

AMP-activated protein kinase (AMPK) is another common downstream effector of α-KG and oligomycin (Chin et al., 2014). AMPK, a key cellular energy sensor, is activated by decreases in cellular energy charge (e.g., upon glucose starvation and many other cellular stress conditions) (Hardie et al., 2012; Zhang et al., 2017). AMPK also elevates autophagy (Galluzzi et al., 2014). Consistent with this understanding, AMPK-dependent beclin 1 phosphorylation on S91 (Kim et al., 2013) was increased in mouse skin treated with α-KG and oligomycin (Figures 1E and 2E). Furthermore, as shown in Figures 3A–3D, anagen induction and hair regeneration were also stimulated by topical treatment with the AMPK activator 5-aminoimidazole-4-carboxamide ribonucleotide (AICAR), an AMP analog. Metformin, another agonist of AMPK (Burkewitz et al., 2014), has been widely used as a diabetes drug and was the first drug approved for human anti-aging studies (Knowler et al., 2002; Barzilai et al., 2016). Here we show that topical metformin similarly induced autophagy and hair regeneration (Figures 3E–3H). Interestingly, although metformin has not been used to study hair growth or treat hair loss, decreased hair loss in polycystic ovary syndrome patients treated with metformin tablets has been documented (Ou et al., 2016; Shahebrahimi et al., 2016).

Mechanistically, metformin has been shown to inhibit mitochondrial complex I in the electron transport chain (Owen et al., 2000; Wheaton et al., 2014). Interestingly, long-lived *C. elegans* mitochondrial mutants accumulate various alpha-keto acid metabolites in the exometabolome (Butler et al., 2010). We previously found that one of these compounds, α-KB, extends the lifespan and alleviates many aging-related symptoms in the aged mice (Huang et al., 2016). α-KB supplementation in drinking water over 30 weeks greatly improved hair coating in old mice (Figures 3I and 3J). However, in pilot experiments testing topical treatments on aged mice, topical α-KB treatment only moderately promoted hair growth in shaved aged animals, whereas topical α-KG or rapamycin did not visibly increase (or even slightly decreased, if it changed at all) hair regeneration (data not shown). In contrast, in young mice, like α-KG and rapamycin treatments, topical α-KB treatment substantially induced skin pigmentation and hair regeneration (Figures 3K–3M). Autophagy was also induced, as

indicated by elevated LC3 and phosphorylated beclin 1 in the treated skin (Figure 3N).

mTOR has previously been reported to be required for hair follicle stem cell activation and anagen entry (Castilho et al., 2009; Kellenberger and Tauchi, 2013; Deng et al., 2015). However, our results above indicate that moderate inhibition of mTOR by rapamycin accompanied by autophagy induction stimulates hair regeneration. Such a dichotomy may also exist for mitochondrial regulation. Mitochondrial respiration is required for hair follicle stem cell cycle and yet genetic perturbation of mitochondrial function abolishes hair regeneration (Hamanaka et al., 2013; Shyh-Chang et al., 2013; Kloepper et al., 2015). Our finding that the well-established complex V inhibitor oligomycin in fact promotes hair regeneration suggested that possibly, as in lifespan regulation, mild mitochondrial inhibition may prove to be beneficial. Because mitochondrial complex V acts upstream of TOR from *C. elegans* to *Drosophila* and humans (Chin et al., 2014; Sun et al., 2014; Fu et al., 2015), and autophagy is induced both by mitochondrial complex V inhibition and by TOR inhibition (Figure 2E) (see also Chin et al., 2014), we decided to determine if autophagy induction alone may be sufficient to elicit hair regeneration.

We took advantage of a TOR-independent autophagy-inducing small molecule, SMER28 (Sarkar et al., 2007), to test our hypothesis that autophagy induction alone would elicit hair regeneration. Topical SMER28 administration increased autophagic induction of LC3 and p62 in mouse dorsal skin (Figures 4A and 4B; Figure S1F). The level of beclin 1 Ser14 phosphorylation, which depends on mTOR (Russell et al., 2013), was not increased in SMER28-treated skin (Figure 4B), indicating an mTOR-independent autophagy-inducing effect by SMER28. Additionally, SMER28 did not appear to induce autophagy by impinging on AMPK, as beclin 1 S91 phosphorylation was also not increased in SMER28-treated skin (Figure 4B). Strikingly, SMER28 also greatly induced hair regeneration (Figure 4C). These findings strongly support the role of autophagy in promoting hair regeneration. To examine whether autophagy is necessary for SMER28-stimulated hair regeneration, we employed autophinib, which inhibits VPS34 and autophagosome formation (Robke et al., 2017). Co-treatment with autophinib prevented hair regeneration by SMER28 (Figure 4D), indicating a critical role of autophagy in hair regeneration. Likewise, autophagy is also necessary for the stimulation of hair regeneration by α-KG (Figure S3) as shown by co-treatments with autophinib, as well as with bafilomycin A1, which disrupts autophagic flux by inhibiting vacuolar H(+)-ATPase (V-ATPase)-dependent acidification and Ca-P60A/SERCA-dependent autophagosome-lysosome fusion (Mauvezin and Neufeld, 2015).

In summary, we showed that inducing autophagy is necessary and sufficient to initiate hair follicle activation and hair regeneration. To understand whether autophagy may be integral to the natural hair follicle cycle, we followed autophagy over different hair follicle stages. We discovered that indeed autophagy is elevated as the hair follicle progresses naturally through anagen; autophagy decreases in catagen and remains low in telogen (Figure 5). These data indicate a biological role of autophagy in normal hair growth initiation and elongation. Consistent with this idea, autophagy has been implicated in maintaining anagen,
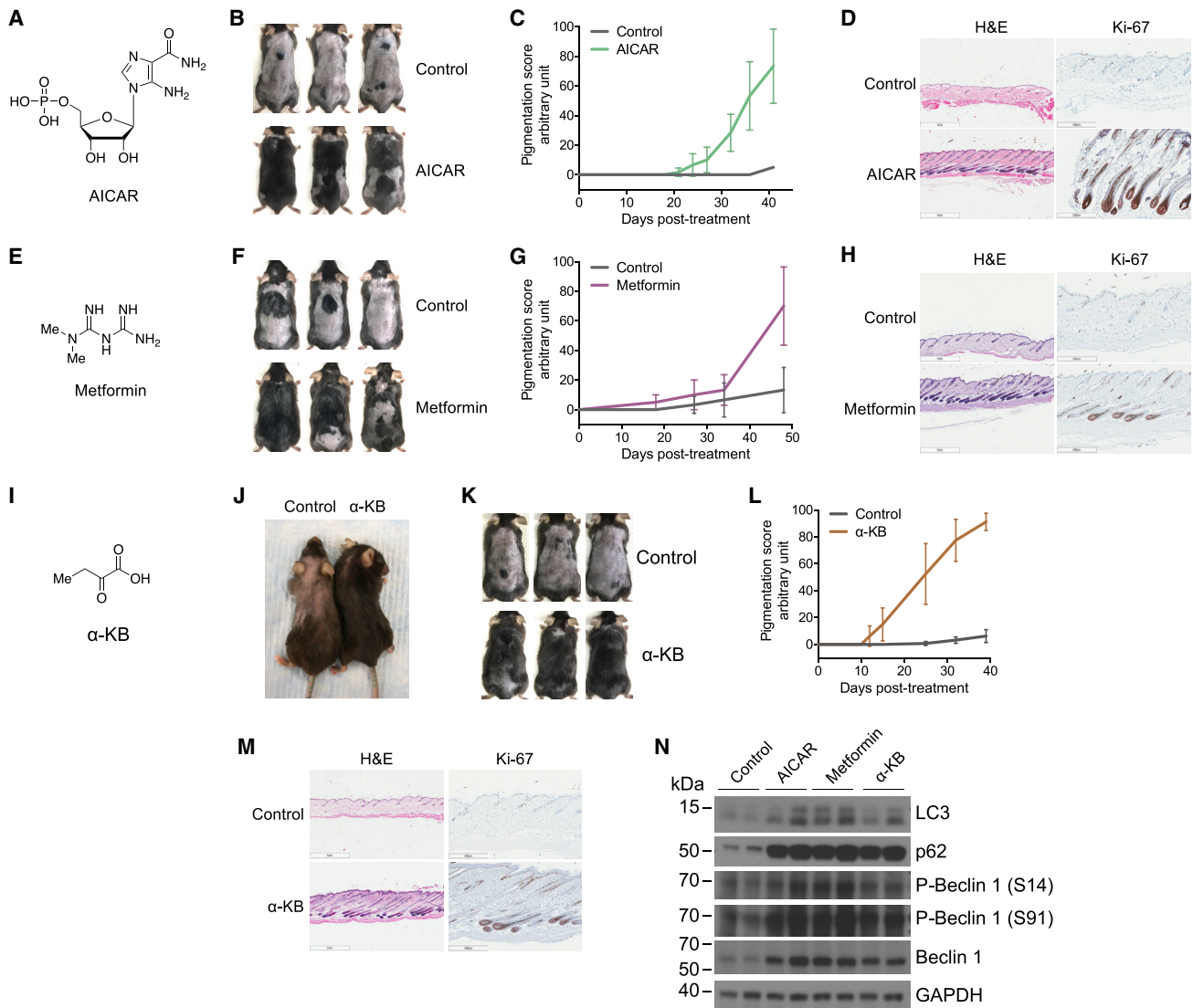
Figure 3. Hair Regeneration Is Induced by AICAR, Metformin, and α-KB

(A) Structure of AICAR.

(B) AICAR (16 mM) induces hair regeneration. Male mice were shaved on postnatal day 44 and treated topically every other day. Photographs were taken on day 41 post-treatment. Number of animals: control, n = 11; AICAR, n = 9. Similar effects in females (not shown).

(C) Quantification for skin pigmentation in mice from (B). Number of animals: control, n = 3; AICAR, n = 3. Data are represented as means ± SD.

(D) H&E- and Ki-67-stained skin tissue section from mice treated with 16 mM AICAR. Scale bars for H&E, 1 mm; scale bars for Ki-67, 400 μm.

(E) Structure of metformin.

(F) Metformin (160 mM) induces hair regeneration. Male mice were shaved on postnatal day 43 and treated topically every other day with metformin or vehicle control (H$_2$O in this experiment). Photographs were taken on day 48 post-treatment. Number of animals: control, n = 13; metformin, n = 12. Similar effects in females (not shown).

(G) Quantification for skin pigmentation in mice from (F). Number of animals: control, n = 3; metformin, n = 3. Data are represented as means ± SD.

(H) H&E- and Ki-67-stained skin tissue section from mice shown in (F). Scale bars for H&E, 1 mm; scale bars for Ki-67, 400 μm.

(I) Structure of α-KB.

(J) Oral α-KB (8 mM in drinking water) treatment negates hair loss in aged female mice. Photo was taken at 131 weeks of age. Number of animals: control, n = 5; α-KB, n = 5.

(K) Topical α-KB (32 mM) induces hair regeneration in young male mice. Mice were shaved on postnatal day 44 and treated topically every other day. Photographs were taken on day 39 post-treatment. Number of animals: control, n = 18; α-KB, n = 18. Similar effects in females (not shown).

(L) Quantification for skin pigmentation in mice from (K). Number of animals: control, n = 4; α-KB, n = 4. Data are represented as means ± SD.

(M) H&E- and Ki-67-stained skin tissue section from mice treated with 32 mM α-KB. Scale bars for H&E, 1 mm; scale bars for Ki-67, 400 μm.

(N) Western blot analysis of autophagy-related markers in telogen skin of mice treated 5 days with indicated compounds.
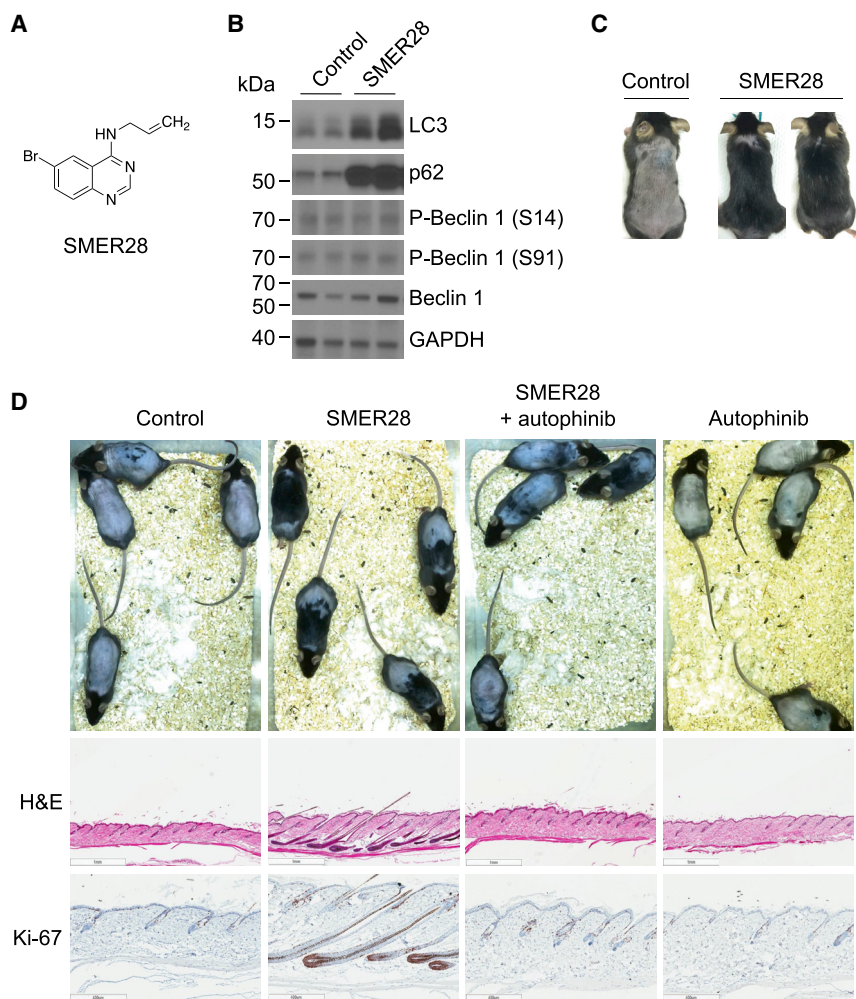
A

SMER28

B

kDa	Control	SMER28	
15 —			LC3
50 —			p62
70 —			P-Beclin 1 (S14)
70 —			P-Beclin 1 (S91)
70 — 50 —			Beclin 1
40 —			GAPDH

C

Control SMER28

Figure 4. SMER28 Induces Hair Regeneration in an Autophagy-Dependent Manner

(A) Structure of SMER28.

(B) Western blot analysis of autophagy-related markers in telogen skin of mice treated 5 days with 1 mM SMER28. Each lane is from a separate mouse.

(C) Male mice were shaved on postnatal day 45 and treated daily with 1 mM SMER28; photographs were taken on day 23 post-treatment. Every other day treatment demonstrated similar results (not shown). Number of animals: control, n = 6; SMER28, n = 6. Similar effects were observed in females (not shown).

(D) SMER28 (2 mM) induced hair regeneration is inhibited by co-treatment with autophinib (4 mM). Mice were shaved on postnatal day 51 and topically treated every other day. Photographs were taken on day 20 post-treatment; histology of corresponding skin tissue section was shown. Scale bars for H&E, 1 mm; scale bars for Ki-67, 400 μm. Number of animals: control n = 20; SMER28, n = 16; SMER28 + autophinib, n = 7; autophinib, n = 7.

See also Figure S3.

D

Control SMER28 SMER28 + autophinib Autophinib

H&E

Ki-67

as autophagy inhibition by knocking down ATG5 in *ex vivo* human anagen hair follicles prematurely induces catagen (Parodi et al., 2018). It remains open which cells are critical for the stimulating effects of the hair regeneration agents. In anagen, hair matrix keratinocytes of organ-cultured human hair follicles exhibit an active autophagic flux (Parodi et al., 2018). As it was postulated that human dermal adipocytes adjacent to catagen hair follicles undergo autophagic degradation of intracellular lipid droplets, communication between hair follicles and dermal white adipose tissue may also be important for hair regeneration (Nicu et al., 2019).

DISCUSSION

The regulation of hair regeneration by microenvironment, including Wnt, BMP, JAK-STAT, Treg, and interleukin-2 receptor signaling, has been widely studied, but little is known about its regulation by intracellular metabolic signals (Ito et al., 2007; Harel et al., 2015; Chueh et al., 2013). Previously cellular redox (Hamanaka et al., 2013), mitochondrial integrity, and energy production (Shyh-Chang et al., 2013; Kloepper et al., 2015) have been

shown to be involved in hair follicle stem cell activation during normal hair growth cycles, which are impaired or dysregulated during aging. Here we have shown that simply treating telogen skin with specific autophagy-inducing small molecules is sufficient to establish anagen and promote hair regeneration.

Rapid anagen entry on whole dorsal telogen skin was observed from time to time among mice treated with α-KG, oligomycin, rapamycin, and SMER28, but never in α-KB-, metformin-, or AICAR-treated mice, nor in vehicle control mice. Temporally, pigmentation (anagen entry) induction by α-KB, AICAR, or metformin takes much longer (e.g., on a time scale of 12–18 days, compared with 5–14 days by α-KG, oligomycin, or rapamycin). It is possible that this may reflect a differential effect by mTOR inhibition and by AMPK activation on the regulation of autophagy; these possibilities remain to be examined. The crosstalk between metabolism and autophagy is complex (Galluzzi et al., 2014). Autophagy is generally induced by limitations in ATP availability or a lack of essential nutrients, including glucose and amino acids, yet ATP is required for autophagy. Starvation and ensuing decreased energy charge and increased ROS levels are potent activators of autophagy. Recently it was reported that calorie restriction also promotes hair follicle growth and retention in mice (Forni et al., 2017) but the underlying mechanism was unclear. It is tempting to speculate that this effect of calorie restriction on hair growth may also be mediated through autophagy activation. In line with this idea, it is conceivable that molecules such as α-KG, rapamycin, and metformin, which may function as calorie restriction (or dietary restriction) mimetics, decrease energy metabolism, reducing skin temperature and inducing hair growth as a defense mechanism against heat loss.
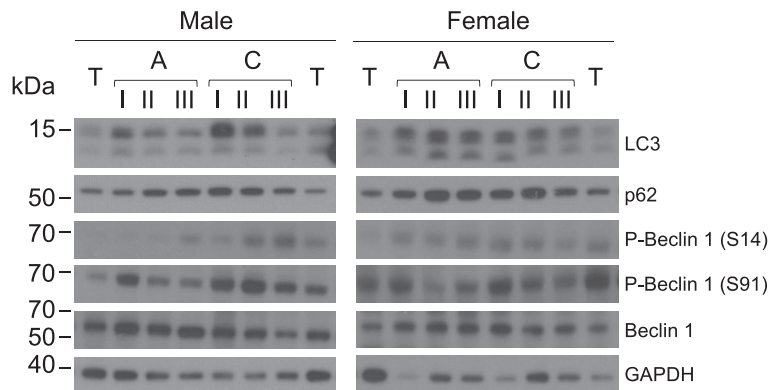
Figure 5. Autophagy Levels Are Indicative of Hair Follicle Cycle Stages, Increased upon Anagen Induction
Mice were shaved on postnatal day 93 for males and on postnatal day 92 for females and monitored for hair cycle progression. Mice at each indicated stage were sacrificed for western blot analysis of autophagy markers. A, anagen; C, catagen; T, telogen.

Autophagy has been linked to longevity, but the underlying mechanisms are unclear. Although autophagy alone may not be sufficient for lifespan increase, many longevity pathways at least partially depend on the induction of autophagy to increase lifespan (Jia and Levine, 2007; Hansen et al., 2008) and lifespan and health-span extension in mice with increased basal autophagy was recently reported (Fernández et al., 2018). Disrupted autophagy has been linked to neurodegenerative diseases, cancer, and other age-related disorders. Given the conservation in energy metabolism and autophagy machinery, induction of hair regeneration by autophagy activation discovered in mice herein should translate to humans. Although it has not been tested in human hair regeneration studies, autophagy has been shown to be essential to maintaining the growth of an *ex vivo* human scalp hair follicle organ culture (Parodi et al., 2018).

It also remains to be studied whether the same autophagy modulators could be useful for treating hair loss patients. Our data show stimulation of hair regeneration in the telogen phase but have not been tested for hair regeneration in alopecia. Although our study did not use a model for alopecia, the findings are relevant to hair loss in the following way. First, hair regeneration, which occurs cyclically under normal conditions but fails in alopecia, would require reactivation of dormant hair follicle stem cells. In our experiments, because mice were shaved in telogen, all hair follicles from the previous cycle were in a resting phase. We find that pharmacological induction of autophagy is sufficient to activate these quiescent telogen hair follicles, when natural anagen-inducing signal(s) are absent, and initiate new anagen and hair regeneration. This suggests that hair loss (e.g., due to lengthened telogen phase, shortened anagen phase, and/or hampered anagen induction) may also be rescued by pharmacologically activating autophagy. Further consistent with this idea, increased autophagy is detected upon anagen entry during the natural hair follicle cycle, and aged mice fed the autophagy- and anagen-inducing metabolite α-KB are protected from hair loss.

STAR★METHODS

Detailed methods are provided in the online version of this paper and include the following:

- KEY RESOURCES TABLE
- CONTACT FOR REAGENT AND RESOURCE SHARING
- EXPERIMENTAL MODEL AND SUBJECT DETAILS
  - ○ Mice
- METHOD DETAILS
  - ○ Assay for hair growth in mice
  - ○ Aged mice
  - ○ Histology and microscopy
  - ○ Western blotting
  - ○ Quantitative reverse transcription PCR
- QUANTIFICATION AND STATISTICAL ANALYSIS

AUTHOR CONTRIBUTIONS

Conceptualization, M.C. and J.H.; Methodology, M.C., M.J., L.V., K.R., and J.H.; Investigation, M.C., M.J., L.V., X.F., and N.B.D.; Validation, M.C., W.H., and J.C.; Formal Analysis, M.C., L.V., and J.H.; Resources, M.J., L.V., S.C.B., J.J., H.H., G.M.C., and K.R.; Writing – Original Draft, M.C. and J.H.; Writing – Review & Editing, M.C., L.V., H.H., G.M.C., K.R., and J.H.; Visualization, M.C. and J.H.; Supervision, J.H.; Funding Acquisition, G.M.C., K.R., and J.H.

DECLARATION OF INTERESTS

UCLA has filed patent applications on the basis of this work, on which M.C., M.J., L.V., X.F., S.C.B., G.M.C., K.R., and J.H. are named as inventors. J.H. is a founder of LongLifeRx Inc. and a member of its scientific advisory board.

REFERENCES

Barzilai, N., Crandall, J.P., Kritchevsky, S.B., and Espeland, M.A. (2016). Metformin as a tool to target aging. Cell Metab. 23, 1060–1065.

Belleudi, F., Purpura, V., Caputo, S., and Torrisi, M.R. (2014). FGF7/KGF regulates autophagy in keratinocytes: a novel dual role in the induction of both assembly and turnover of autophagosomes. Autophagy 10, 803–821.

Burkewitz, K., Zhang, Y., and Mair, W.B. (2014). AMPK at the nexus of energetics and aging. Cell Metab. 20, 10–25.

Butler, J.A., Ventura, N., Johnson, T.E., and Rea, S.L. (2010). Long-lived mitochondrial (Mit) mutants of Caenorhabditis elegans utilize a novel metabolism. FASEB J. 24, 4977–4988.

Castilho, R.M., Squarize, C.H., Chodosh, L.A., Williams, B.O., and Gutkind, J.S. (2009). mTOR mediates Wnt-induced epidermal stem cell exhaustion and aging. Cell Stem Cell 5, 279–289.

Chikh, A., Sanzà, P., Raimondi, C., Akinduro, O., Warnes, G., Chiorino, G., Byrne, C., Harwood, C.A., and Bergamaschi, D. (2014). iASPP is a novel autophagy inhibitor in keratinocytes. J. Cell Sci. 127, 3079–3093.

Chin, R.M., Fu, X., Pai, M.Y., Vergnes, L., Hwang, H., Deng, G., Diep, S., Lomenick, B., Meli, V.S., Monsalve, G.C., et al. (2014). The metabolite α-ketoglutarate extends lifespan by inhibiting ATP synthase and TOR. Nature 510, 397–401.

Chueh, S.C., Lin, S.J., Chen, C.C., Lei, M., Wang, L.M., Widelitz, R., Hughes, M.W., Jiang, T.X., and Chuong, C.M. (2013). Therapeutic strategy for hair regeneration: hair cycle activation, niche environment modulation, wound-induced follicle neogenesis, and stem cell engineering. Expert Opin. Biol. Ther. 13, 377–391.

Cuervo, A.M., and Dice, J.F. (2000). Age-related decline in chaperone-mediated autophagy. J. Biol. Chem. 275, 31505–31513.

Deng, Z., Lei, X., Zhang, X., Zhang, H., Liu, S., Chen, Q., Hu, H., Wang, X., Ning, L., Cao, Y., et al. (2015). mTOR signaling promotes stem cell activation via counterbalancing BMP-mediated suppression during hair regeneration. J. Mol. Cell Biol. 7, 62–72.

Fernández, A.F., Sebti, S., Wei, Y., Zou, Z., Shi, M., McMillan, K.L., He, C., Ting, T., Liu, Y., Chiang, W.C., et al. (2018). Disruption of the beclin 1-BCL2 autophagy regulatory complex promotes longevity in mice. Nature 558, 136–140.

Forni, M.F., Peloggia, J., Braga, T.T., Chinchilla, J.E.O., Shinohara, J., Navas, C.A., Camara, N.O.S., and Kowaltowski, A.J. (2017). Caloric restriction promotes structural and metabolic changes in the skin. Cell Rep. 20, 2678–2692.

Fu, X., Chin, R.M., Vergnes, L., Hwang, H., Deng, G., Xing, Y., Pai, M.Y., Li, S., Ta, L., Fazlollahi, F., et al. (2015). 2-Hydroxyglutarate inhibits ATP synthase and mTOR signaling. Cell Metab. 22, 508–515.

Galluzzi, L., Pietrocola, F., Levine, B., and Kroemer, G. (2014). Metabolic control of autophagy. Cell 159, 1263–1276.

Gilhar, A., Etzioni, A., and Paus, R. (2012). Alopecia areata. N. Engl. J. Med. 366, 1515–1525.

Hamanaka, R.B., Glasauer, A., Hoover, P., Yang, S., Blatt, H., Mullen, A.R., Getsios, S., Gottardi, C.J., DeBerardinis, R.J., Lavker, R.M., and Chandel, N.S. (2013). Mitochondrial reactive oxygen species promote epidermal differentiation and hair follicle development. Sci. Signal. 6, ra8.

Hansen, M., Chandra, A., Mitic, L.L., Onken, B., Driscoll, M., and Kenyon, C. (2008). A role for autophagy in the extension of lifespan by dietary restriction in C. elegans. PLoS Genet. 4, e24.

Hardie, D.G., Ross, F.A., and Hawley, S.A. (2012). AMPK: a nutrient and energy sensor that maintains energy homeostasis. Nat. Rev. Mol. Cell Biol. 13, 251–262.

Harel, S., Higgins, C.A., Cerise, J.E., Dai, Z., Chen, J.C., Clynes, R., and Christiano, A.M. (2015). Pharmacologic inhibition of JAK-STAT signaling promotes hair growth. Sci. Adv. 1, e1500973.

Hirano, T., Akira, S., Taga, T., and Kishimoto, T. (1990). Biological and clinical aspects of interleukin 6. Immunol. Today 11, 443–449.

Ho, T.T., Warr, M.R., Adelman, E.R., Lansinger, O.M., Flach, J., Verovskaya, E.V., Figueroa, M.E., and Passegué, E. (2017). Autophagy maintains the metabolism and function of young and old stem cells. Nature 543, 205–210.

Huang, J., Chin, R., Fu, X., Hwang, H., Reue, K., Vergnes, L., Jiang, M., Lomenick, B.E., Yin, X., Eghbali, M., et al. (2016). Ketobutyrate compounds and compositions for treating age-related symptoms and diseases. https://patents.google.com/patent/WO2016003854A1.

Ito, M., Yang, Z., Andl, T., Cui, C., Kim, N., Millar, S.E., and Cotsarelis, G. (2007). Wnt-dependent de novo hair follicle regeneration in adult mouse skin after wounding. Nature 447, 316–320.

Jia, K., and Levine, B. (2007). Autophagy is required for dietary restriction-mediated life span extension in C. elegans. Autophagy 3, 597–599.

Kabeya, Y., Mizushima, N., Ueno, T., Yamamoto, A., Kirisako, T., Noda, T., Kominami, E., Ohsumi, Y., and Yoshimori, T. (2000). LC3, a mammalian homologue of yeast Apg8p, is localized in autophagosome membranes after processing. EMBO J. 19, 5720–5728.

Kellenberger, A.J., and Tauchi, M. (2013). Mammalian target of rapamycin complex 1 (mTORC1) may modulate the timing of anagen entry in mouse hair follicles. Exp. Dermatol. 22, 77–80.

Keyes, B.E., Segal, J.P., Heller, E., Lien, W.H., Chang, C.Y., Guo, X., Oristian, D.S., Zheng, D., and Fuchs, E. (2013). Nfatc1 orchestrates aging in hair follicle stem cells. Proc. Natl. Acad. Sci. U S A 110, E4950–E4959.

Kim, J., Kim, Y.C., Fang, C., Russell, R.C., Kim, J.H., Fan, W., Liu, R., Zhong, Q., and Guan, K.L. (2013). Differential regulation of distinct Vps34 complexes by AMPK in nutrient stress and autophagy. Cell 152, 290–303.

Kloepper, J.E., Baris, O.R., Reuter, K., Kobayashi, K., Weiland, D., Vidali, S., Tobin, D.J., Niemann, C., Wiesner, R.J., and Paus, R. (2015). Mitochondrial function in murine skin epithelium is crucial for hair follicle morphogenesis and epithelial-mesenchymal interactions. J. Invest. Dermatol. 135, 679–689.

Knowler, W.C., Barrett-Connor, E., Fowler, S.E., Hamman, R.F., Lachin, J.M., Walker, E.A., and Nathan, D.M.; Diabetes Prevention Program Research Group (2002). Reduction in the incidence of type 2 diabetes with lifestyle intervention or metformin. N. Engl. J. Med. 346, 393–403.

Levine, B., and Kroemer, G. (2008). Autophagy in the pathogenesis of disease. Cell 132, 27–42.

Liang, X.H., Jackson, S., Seaman, M., Brown, K., Kempkes, B., Hibshoosh, H., and Levine, B. (1999). Induction of autophagy and inhibition of tumorigenesis by beclin 1. Nature 402, 672–676.

Magerl, M., Tobin, D.J., Müller-Röver, S., Hagen, E., Lindner, G., McKay, I.A., and Paus, R. (2001). Patterns of proliferation and apoptosis during murine hair follicle morphogenesis. J. Invest. Dermatol. 116, 947–955.

Mauvezin, C., and Neufeld, T.P. (2015). Bafilomycin A1 disrupts autophagic flux by inhibiting both V-ATPase-dependent acidification and Ca-P60A/SERCA-dependent autophagosome-lysosome fusion. Autophagy 11, 1437–1438.

Messenger, A.G., and Rundegren, J. (2004). Minoxidil: mechanisms of action on hair growth. Br. J. Dermatol. 150, 186–194.

Mizushima, N., Levine, B., Cuervo, A.M., and Klionsky, D.J. (2008). Autophagy fights disease through cellular self-digestion. Nature 451, 1069–1075.

Müller-Röver, S., Handjiski, B., van der Veen, C., Eichmüller, S., Foitzik, K., McKay, I.A., Stenn, K.S., and Paus, R. (2001). A comprehensive guide for the accurate classification of murine hair follicles in distinct hair cycle stages. J. Invest. Dermatol. 117, 3–15.

Nicu, C., Hardman, J.A., Pople, J., and Paus, R. (2019). Do human dermal adipocytes switch from lipogenesis in anagen to lipophagy and lipolysis during catagen in the human hair cycle? Exp. Dermatol. 28, 432–435.

Ohsumi, Y. (2014). Historical landmarks of autophagy research. Cell Res. 24, 9–23.

Ou, H.T., Chen, P.C., Wu, M.H., and Lin, C.Y. (2016). Metformin improved health-related quality of life in ethnic Chinese women with polycystic ovary syndrome. Health Qual. Life Outcomes 14, 119.

Owen, M.R., Doran, E., and Halestrap, A.P. (2000). Evidence that metformin exerts its anti-diabetic effects through inhibition of complex 1 of the mitochondrial respiratory chain. Biochem. J. 348, 607–614.

Parodi, C., Hardman, J.A., Allavena, G., Marotta, R., Catelani, T., Bertolini, M., Paus, R., and Grimaldi, B. (2018). Autophagy is essential for maintaining the growth of a human (mini-)organ: Evidence from scalp hair follicle organ culture. PLoS Biol. 16, e2002864.

Petukhova, L., Duvic, M., Hordinsky, M., Norris, D., Price, V., Shimomura, Y., Kim, H., Singh, P., Lee, A., Chen, W.V., et al. (2010). Genome-wide association study in alopecia areata implicates both innate and adaptive immunity. Nature 466, 113–117.

Robke, L., Laraia, L., Carnero Corrales, M.A., Konstantinidis, G., Muroi, M., Richters, A., Winzker, M., Engbring, T., Tomassi, S., Watanabe, N., et al. (2017). Phenotypic identification of a novel autophagy inhibitor chemotype targeting lipid kinase VPS34. Angew. Chem. Int. Ed. Engl. 56, 8153–8157.

Rossiter, H., Stübiger, G., Gröger, M., König, U., Gruber, F., Sukseree, S., Mlitz, V., Buchberger, M., Oskolkova, O., Bochkov, V., et al. (2018). Inactivation of autophagy leads to changes in sebaceous gland morphology and function. Exp. Dermatol. 27, 1142–1151.

Russell, R.C., Tian, Y., Yuan, H., Park, H.W., Chang, Y.Y., Kim, J., Kim, H., Neufeld, T.P., Dillin, A., and Guan, K.L. (2013). ULK1 induces autophagy by phosphorylating Beclin-1 and activating VPS34 lipid kinase. Nat. Cell Biol. 15, 741–750.

Sahani, M.H., Itakura, E., and Mizushima, N. (2014). Expression of the autophagy substrate SQSTM1/p62 is restored during prolonged starvation depending on transcriptional upregulation and autophagy-derived amino acids. Autophagy 10, 431–441.

Salemi, S., Yousefi, S., Constantinescu, M.A., Fey, M.F., and Simon, H.U. (2012). Autophagy is required for self-renewal and differentiation of adult human stem cells. Cell Res. 22, 432–435.

Sarkar, S., Perlstein, E.O., Imarisio, S., Pineau, S., Cordenier, A., Maglathlin, R.L., Webster, J.A., Lewis, T.A., O'Kane, C.J., Schreiber, S.L., and Rubinsztein, D.C. (2007). Small molecules enhance autophagy and reduce toxicity in Huntington's disease models. Nat. Chem. Biol. 3, 331–338.

Schneider, M.R., Schmidt-Ullrich, R., and Paus, R. (2009). The hair follicle as a dynamic miniorgan. Curr. Biol. 19, R132–R142.

Shahebrahimi, K., Jalilian, N., Bazgir, N., and Rezaei, M. (2016). Comparison clinical and metabolic effects of metformin and pioglitazone in polycystic ovary syndrome. Indian J. Endocrinol. Metab. 20, 805–809.

Shyh-Chang, N., Zhu, H., Yvanka de Soysa, T., Shinoda, G., Seligson, M.T., Tsanov, K.M., Nguyen, L., Asara, J.M., Cantley, L.C., and Daley, G.Q. (2013). Lin28 enhances tissue repair by reprogramming cellular metabolism. Cell 155, 778–792.

Slominski, A., and Paus, R. (1993). Melanogenesis is coupled to murine anagen: toward new concepts for the role of melanocytes and the regulation of melanogenesis in hair growth. J. Invest. Dermatol. 101 (1, Suppl), 90S–97S.

Solanas, G., Peixoto, F.O., Perdiguero, E., Jardí, M., Ruiz-Bonilla, V., Datta, D., Symeonidi, A., Castellanos, A., Welz, P.S., Caballero, J.M., et al. (2017). Aged stem cells reprogram their daily rhythmic functions to adapt to stress. Cell 170, 678–692.e20.

Sun, X., Wheeler, C.T., Yolitz, J., Laslo, M., Alberico, T., Sun, Y., Song, Q., and Zou, S. (2014). A mitochondrial ATP synthase subunit interacts with TOR signaling to modulate protein homeostasis and lifespan in Drosophila. Cell Rep. 8, 1781–1792.

Tang, A.H., and Rando, T.A. (2014). Induction of autophagy supports the bioenergetic demands of quiescent muscle stem cell activation. EMBO J. 33, 2782–2797.

Walpoth, B.H., Pavlicek, M., Celik, B., Nicolaus, B., Schaffner, T., Althaus, U., Hess, O.M., Carrel, T., and Morris, R.E. (2001). Prevention of neointimal proliferation by immunosuppression in synthetic vascular grafts. Eur. J. Cardiothorac. Surg. 19, 487–492.

Wang, H., Peters, T., Kess, D., Sindrilaru, A., Oreshkova, T., Van Rooijen, N., Stratis, A., Renkl, A.C., Sunderkötter, C., Wlaschek, M., et al. (2006). Activated macrophages are essential in a murine model for T cell-mediated chronic psoriasiform skin inflammation. J. Clin. Invest. 116, 2105–2114.

Wang, L., Guo, L.L., Wang, L.H., Zhang, G.X., Shang, J., Murao, K., Chen, D.F., Fan, X.H., and Fu, W.Q. (2015). Oxidative stress and substance P mediate psychological stress-induced autophagy and delay of hair growth in mice. Arch. Dermatol. Res. 307, 171–181.

Wheaton, W.W., Weinberg, S.E., Hamanaka, R.B., Soberanes, S., Sullivan, L.B., Anso, E., Glasauer, A., Dufour, E., Mutlu, G.M., Budigner, G.S., and Chandel, N.S. (2014). Metformin inhibits mitochondrial complex I of cancer cells to reduce tumorigenesis. eLife 3, e02242.

Yoshihara, N., Ueno, T., Takagi, A., Oliva Trejo, J.A., Haruna, K., Suga, Y., Komatsu, M., Tanaka, K., and Ikeda, S. (2015). The significant role of autophagy in the granular layer in normal skin differentiation and hair growth. Arch. Dermatol. Res. 307, 159–169.

Zhang, P., Verity, M.A., and Reue, K. (2014). Lipin-1 regulates autophagy clearance and intersects with statin drug effects in skeletal muscle. Cell Metab. 20, 267–279.

Zhang, C.S., Hawley, S.A., Zong, Y., Li, M., Wang, Z., Gray, A., Ma, T., Cui, J., Feng, J.W., Zhu, M., et al. (2017). Fructose-1,6-bisphosphate and aldolase mediate glucose sensing by AMPK. Nature 548, 112–116.

STAR★METHODS

KEY RESOURCES TABLE

REAGENT or RESOURCE	SOURCE	IDENTIFIER
Antibodies		
Rabbit monoclonal anti-Ki-67 (D3B5)	Cell Signaling Technology	Cat#12202; RRID: AB_2620142
Rabbit polyclonal anti-IL-6	Abcam	Cat#ab6672; RRID: AB_2127460
Rat monoclonal anti-F4/80 (clone Cl:A3-1)	Bio-Rad	Cat#MCA497G; RRID: AB_872005
Rabbit polyclonal anti-LC3B	Novus	Cat#NB100-2220; RRID: 10003146
Rabbit polyclonal anti-p62/SQSTM1 (C-terminal)	Sigma-Aldrich	Cat#P0068; RRID: AB_1841066
Rabbit monoclonal anti-Phospho-Beclin-1 (Ser15) (D4B7R)	Cell Signaling Technology	Cat#84966; RRID: AB_2800045
Rabbit monoclonal anti-Phospho-Beclin-1 (Ser93) (D9A5G)	Cell Signaling Technology	Cat#14717; RRID: AB_2688032
Rabbit monoclonal anti-Beclin 1 [EPR19662]	Abcam	Cat#ab207612; RRID: AB_2692326
Mouse monoclonal anti-GAPDH (6C5)	Thermo Fisher Scientific	Cat#AM4300; RRID: AB_2536381
Chemicals, Peptides, and Recombinant Proteins		
dimethyl sulfoxide	Sigma-Aldrich	D8418; CAS: 67-68-5
α-ketoglutaric acid	Sigma-Aldrich	75890; CAS: 328-50-7
oligomycin	Cell Signaling Technology	9996L; CAS: 1404-19-9
rapamycin	Selleckchem	S1039; CAS: 53123-88-9
AICAR (acadesine)	Selleckchem	S1802; CAS: 2627-69-2
metformin hydrochloride	Sigma-Aldrich	PHR1084; CAS: 1115-70-4
2-ketobutyric acid	Sigma-Aldrich	K401; CAS: 600-18-0
SMER28	Selleckchem	S8240; CAS: 307538-42-7
autophinib	Selleckchem	S8596; CAS: 1644443-47-9
bafilomycin A1	Selleckchem	S1413; CAS: 88899-55-2
premium lecithin organogel (PLO) base	Transderma Pharmaceuticals Inc	Cat#TR201
10% formalin solution	Sigma	Cat#HT501128
T-PER tissue protein extraction buffer	Thermo Scientific	Cat#78510
cOmplete, mini protease inhibitor cocktail	Roche	Cat#11836153001
phosphatase inhibitor cocktail 2	Sigma-Aldrich	Cat#P5726
sodium dodecyl sulfate (SDS)	Thermo Fisher Scientific	Cat#BP166; CAS: 151-21-3
β-mercaptoethanol	Thermo Fisher Scientific	Cat# O3446I-100; CAS: 60-24-2
20X Bolt MOPS SDS running buffer	Invitrogen	Cat#B0001
TRIzol reagent	Invitrogen	Cat#15596026
Critical Commercial Assays		
Lysing matrix A tubes	MP Biomedicals	Cat#116910100
NuPAGE 12% Bis-Tris protein gels, 1.0 mm, 15-well	Invitrogen	Cat#NP0343BOX
Immobilon-P PVDF membrane	Millipore	Cat# IPVH00010
iScript reverse transcription supermix	Bio-Rad	Cat#1708840
iTaq universal SYBR Green supermix	Bio-Rad	Cat#172-5120
Experimental Models: Organisms/Strains		
Mouse: C57BL/6J	Jackson Laboratories	JAX: 000664, RRID:IMSR_JAX:000664
Mouse: C57BL/6J at the age of 87 weeks or 21 months	NIA aged rodent colonies	N/A
Oligonucleotides		
Primers: p62 forward: GAAGAATGTGGGGGAGAGTGTGG; reverse: TGCCTGTGCTGGAACTTTCTGG	Zhang et al., 2014	N/A

Continued

REAGENT or RESOURCE	SOURCE	IDENTIFIER
Primers: B2m forward: CAGCATGGCTCGCTCGGTGAC; reverse: CGTAGCAGTTCAGTATGTTCG	This paper	N/A
Software and Algorithms		
GraphPad Prism	GraphPad Software	RRID: SCR_002798
Microsoft Excel	Microsoft	RRID: SCR_016137

CONTACT FOR REAGENT AND RESOURCE SHARING

Further information and requests for resources and reagents should be directed to and will be fulfilled by the Lead Contact, Jing Huang (jinghuang.ucla@gmail.com).

EXPERIMENTAL MODEL AND SUBJECT DETAILS

Mice

All experiments were approved by the UCLA Chancellor's Animal Research Committee. Mice were housed (up to 4 animals per cage) in a controlled SPF facility ($22 \pm 2°C$, 6:00-18:00, 12 h/12 h light/dark cycle) at UCLA. Mice were fed a standard chow diet and provided *ad libitum* access to food and water throughout the study. C57BL/6J male mice were obtained at 6 or 8 weeks of age from Jackson Laboratories (Bar Harbor, ME). C57BL/6J female mice were obtained at 8 weeks of age from Jackson Laboratories (Bar Harbor, ME). For oral α-KB treatment, aged male and female C57BL/6J mice were obtained at 87 weeks of age (NIA aged rodent colonies). For topical α-KB treatment, aged male C57BL/6J mice were obtained at 21 months of age (NIA aged rodent colonies). In all experiments, age- and sex-matched animals were randomized into control and treatment groups.

METHOD DETAILS

Assay for hair growth in mice

All compounds were tested in both male and female mice. Every experiment was repeated independently at least 2 times. Some treatments with different agents were performed concurrently with shared control arms. C57BL/6J mice were obtained from Jackson Laboratories (Bar Harbor, ME) at 6 or 8 weeks of age for males and at 8 weeks of age for females. Mice were shaved dorsally in telogen, i.e., postnatal day 43~45 for males (unless otherwise indicated) and day 58 for females, respectively. Vehicle control (25 μL DMSO, unless otherwise indicated) or test compounds (in 25 μL DMSO, unless otherwise indicated) were topically applied on the shaved skin every other day (unless otherwise described) for the duration of the experiments (3-6 weeks). Appearance of skin pigmentation and hair growth were monitored and documented by photos and videos, with the experimenter(s) being blind to the treatment conditions. Progression was also assigned a value from 0 to 100 based on pigmentation levels and hair shaft density, with 0 indicating no hair growth (and no pigmentation) and higher number corresponding to darker skin and larger areas of dense hair growth. Scoring was done blindly. Images representing different scores are presented in Figure S4. DMSO (Sigma), α-KG (Sigma), oligomycin (Cell Signaling), rapamycin (Selleckchem), AICAR (Selleckchem), metformin (Sigma), α-KB (Sigma), SMER28 (Selleckchem), autophinib (Selleckchem), bafilomycin A1 (Selleckchem), or indicated combinations in ~250 μL Premium Lecithin Organogel (PLO) Base (Transderma Pharmaceuticals Inc.) were used for each mouse. The vehicle DMSO was also mixed with PLO base for topical application. The timing of the hair cycle was not altered using PLO base +DMSO versus PLO base alone in our experiments.

Aged mice

For oral α-KB treatment, aged male and female C57BL/6J mice were randomly assigned to treatment with either drinking water (vehicle control) or α-KB (90 mg/kg bodyweight) in drinking water, started when mice were at 101 weeks of age. For topical α-KB treatment, aged male C57BL/6J mice were obtained at 21 months of age (NIA aged rodent colonies), shaved the following week, and randomly assigned to be topically treated with either α-KB (32 mM) or vehicle control every other day for one month.

Histology and microscopy

C57BL/6J mouse dorsal skin was shaved before being collected for histological and molecular analyses. Full-thickness skin tissue was then fixed in 10% formalin solution (Sigma) overnight and dehydrated for embedding in paraffin. 5 μm paraffin sections were subjected to hematoxylin/eosin staining and immunohistochemistry. Antibodies used are listed in the key resources table. Images were captured by Leica Aperio ScanScope AT brightfield system at X20 magnification.

Western blotting

Male C57BL/6J mice were shaved and treated every other day starting on postnatal day 43. After 5 days (unless otherwise indicated), telogen skin samples were harvested and stage confirmed. Mouse skin tissue lysate was prepared by homogenization in T-PER Tissue Protein Extraction Buffer (Thermo Scientific) with protease inhibitors (Roche) and phosphatase inhibitors (Sigma) by FastPrep-24 (MP Biomedicals) in Lysing Matrix A tubes (MP Biomedicals). Tissue and cell debris was removed by centrifugation and the lysate was boiled for 5 min in 1 x SDS (Fisher Scientific) loading buffer containing 5% β-mercaptoethanol (Fisher Scientific). Samples were then subjected to SDS–PAGE on NuPAGE Novex 12% Bis-Tris gels (Invitrogen) in MOPS SDS Running Buffer (Invitrogen), and transferred to PVDF membranes for western blotting. All antibodies used are listed in the key resources table.

Quantitative reverse transcription PCR

Male C57BL/6J mice on postnatal day 43 were randomly assigned to either control (DMSO), or α-KG or SMER28 treatment groups. At 24 h post-treatment, telogen skin samples were harvested and total RNA was isolated using TRIzol reagent (Invitrogen) from whole thickness mouse skin tissue. cDNA was synthesized using iScript Reverse Transcription Supermix (Bio-Rad). iTaq Universal SYBR Green Supermix (Bio-Rad) and a Bio-Rad CFX Connect instrument were used for quantitative RT-PCR. Primer sequences are listed in the key resources table (Zhang et al., 2014). Relative gene expression was calculated as $2^{-\Delta\Delta CT}$, where beta-2-microglobulin (B2m) was used as the housekeeping gene for normalization.

QUANTIFICATION AND STATISTICAL ANALYSIS

All treatments were repeated at least two times. Data represent biological replicates. Statistical tests used, number of animals, and p values are described in the legend for each figure. Data meet the assumptions of the statistical tests described for each figure. Mean ± s.d. is plotted in all figures.